NDT of Dielectric Material using CPW FED UWB Receiver Antenna and Single Band Sensor Antenna

Sandeep Singh [#1], Mohammad Imroz Khan [#2], Valavoju Mahesh Chary[#3], Sivaramakrishnan S[#4]
Scientist/Engineer-SE[#1,3], Scientist/Engineer-SC[#2] , Deputy General Manager[#4]

[#]Satish Dhawan Space Center, ISRO, Sriharikota, Andhra Pradesh, India – 524124
Email: [1]sandeep.singh@shar.gov.in, [2]imroz.khan@shar.gov.in, [3]mahesh.chary@shar.gov.in, [4]sivaramakrishnan.s@shar.gov.in

Abstract

This paper presents a simulation model for carrying out non-destructive evaluation of relative permittivity for dielectric materials using dual antenna setup. The proposed model involves coplanar waveguide fed single band sensor antenna and an ultra wideband receiver antenna. The sensor antenna consists of a single resonating band and is mounted on the surface of the test material. An ultra-wideband antenna is placed in the far field region of the sensor antenna inorder to capture the frequencies radiated by the sensor antenna. The working principle of the proposed concept lies in the fact that the resonating frequency of the sensor antenna is a function of relative permittivity of the dielectric material under test. The designed sensor antenna radiates at a particular known frequency when mounted on the surface of the test material of known permittivity. This frequency radiated by sensor antenna is captured by ultra wideband antenna and any shift in the resonating band of the sensor antenna can easily be detected. Thus any shift in resonating band for sensor antenna will directly reflect the change in the permittivity value of the test material. The proposed sensor antenna has resonating band with center frequency at 5 GHz, while the ultra wideband antenna covers the entire frequency sweep from 3 - 12 GHz.

Keywords: *CPW, dielectric, non-destructive testing, patch antenna, sensor antenna, UWB antenna*

I. INTRODUCTION

The use of microwave spectrum for non destructive testing (NDT) of materials has become quite prominent since last two decades. Mechanism for detection of surface cracks and air voids have been readily implemented using microwave frequency. In [1] a leaky wave antenna is studied which is operating in X band, in [2] mechanical scanner is integrated with vector network analyzer in order to detect the change in frequency due to variation in permittivity of test material, in [3] subsurface radar is implemented, in [4] antenna array of multiple dipole antennas for microwave imaging is studied, in [5] open ended waveguide is studied for evaluating dielectric properties.

In this document a dual antenna setup is modelled using CST Microwave Studio for non destructive evaluation of relative permittivity of dielectric material. The proposed antenna setup comprises of two coplanar waveguide (CPW) fed patch antennas, namely, sensor antenna and receiver antenna. The sensor antenna is a single band planar antenna which can be mounted on the surface of the test material of known permittivity. An ultra-wideband (UWB) antenna is placed in the far field of the sensor antenna for capturing the frequencies radiated by the sensor antenna. Since, the sensor antenna is modelled with respect to the permittivity of the test material, hence, it will be resonating at a particular known frequency. This frequency radiated by the sensor antenna will be intercepted by the ultra wideband antenna and will be displayed on Vector Network Analyzer (VNA). Since, the resonating band of the sensor antenna is a function of relative permittivity of the test material, hence, any shift in the resonating band of sensor antenna will directly

reflect a change in the permittivity value of the test material.

II. ANTENNA DESIGN AND ANALYSIS

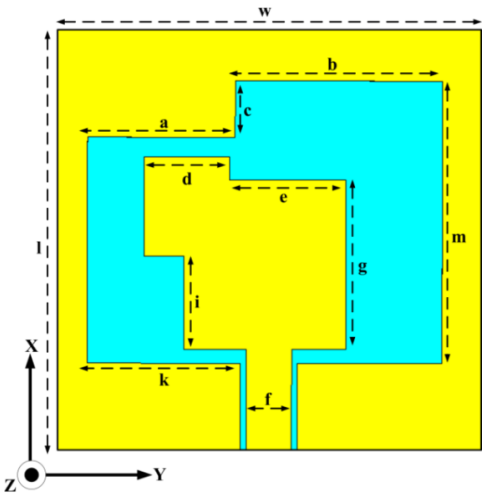

Fig. 1. Geometrical view of proposed sensor antenna

TABLE I. GEOMETRICAL DIMENSIONS OF SENSOR ANTENNA

a	b	c	d	e	f
10.4	14.6	4	6	8.2	3.2
g	l	w	ii	k	m
12	30	30	6.6	10.8	20

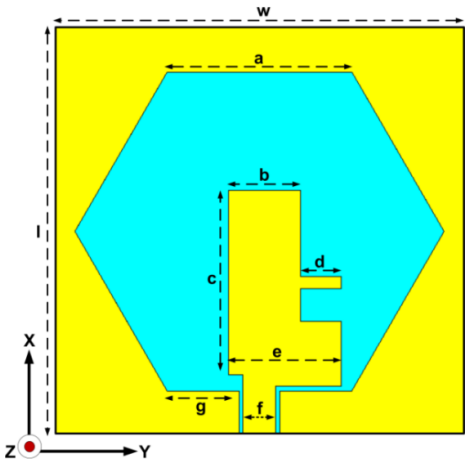

Fig. 2. Geometrical view of proposed UWB receiver antenna

TABLE II. GEOMETRICAL DIMENSIONS OF UWB RECEIVER ANTENNA

a	b	c	d	e	f	g	l	w
18	7	18	4	11	3.2	7	40	40

The geometrical view of the proposed sensor antenna is depicted in fig. 1 along with its physical dimensions illustrated in Table I. Fig. 2 depicts the geometrical view of the proposed ultra wideband antenna whose physical dimensions are displayed by Table II. Both antennas are modelled on CST Microwave Studio with FR4 as substrate.

A. Input Impedance Matching Analysis

Impedance matching at the input feed port of antenna is the most crucial factor for achieving resonant band. The impedance matching analysis is carried out by studying Smith chart plot and voltage standing wave ratio (VSWR) plot. Smith chart for sensor antenna is depicted in fig. 3, while Smith chart for ultra wideband antenna is depicted in fig. 4. VSWR for sensor antenna is illustrated in fig. 5, while for ultra wideband antenna it is illustrated in fig. 6. VSWR value for a resonating band must be less than two. For both the antennas, VSWR value lies below two for the resonating band.

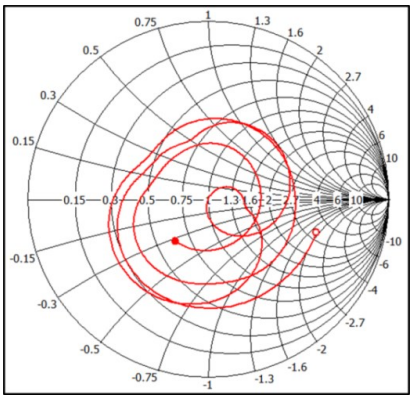

Fig. 3. Smith chart plot for sensor antenna

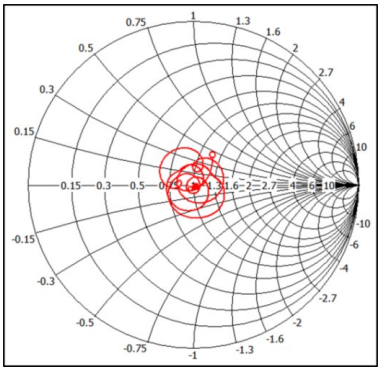

Fig. 4. Smith chart plot for UWB receiver antenna

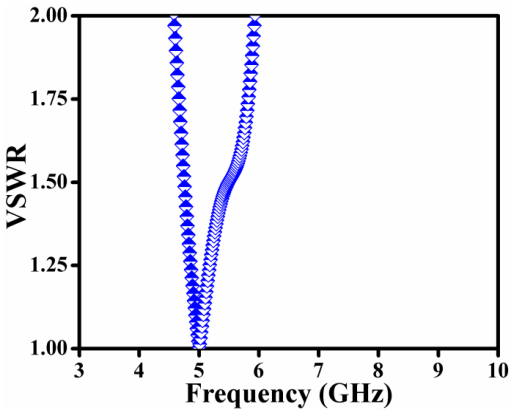

Fig. 5. VSWR of proposed sensor antenna

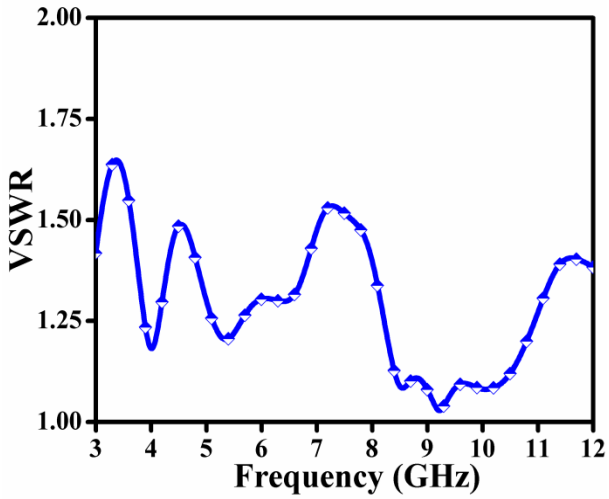

Fig. 6. VSWR of proposed UWB receiver antenna

B. *Proposed Antenna Setup Analysis*

The dual antenna model for non destructive evaluation of dielectric constant of the test material is analyzed in this section. The side view of the sensor antenna mounted on the test material is depicted in fig. 7. The sensor antenna mounted on the test material has three layers, namely, copper (yellow layer), FR4 substrate (blue layer) and test material (red layer). The schematic diagram for the proposed antenna setup is illustrated in fig. 8.

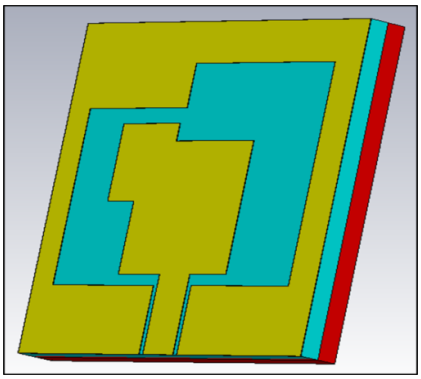

Fig. 7. Sensor antenna mounted on the surface of test material

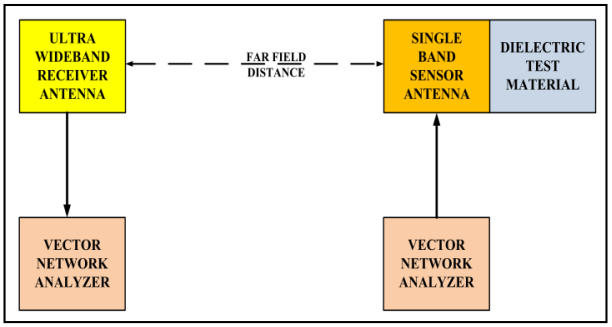

Fig. 8. Schematic view of proposed antenna setup

C. *Surface Current And Mode Analysis*

Surface current distribution for antenna with advancing time illustrates the antenna regions responsible for major radiation. Surface current distribution for sensor antenna is shown in fig. 9, which confirms that the patch as well as ground plane are contributing to radiation. Fig. 10 depicts surface current distribution for ultra wideband antenna which illustrates that the active patch is the major contributor for the radiation. Subsequently, fig. 11 and fig. 12 shows the modes generated in the coplanar waveguide antenna with respect to advancing time.

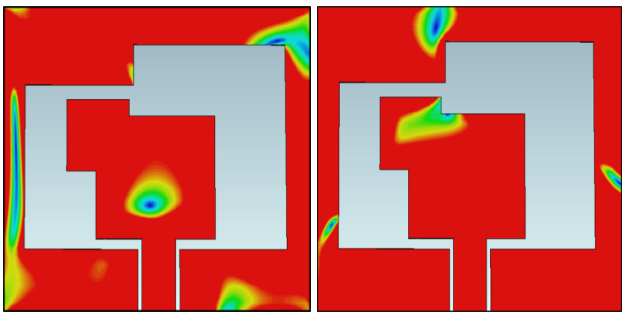

t = 0 t = T/4

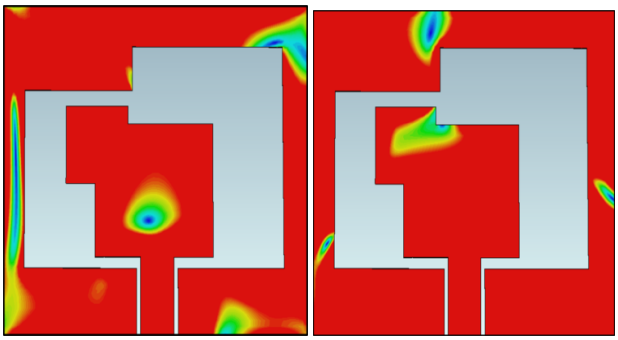

t = T/2 t = 3T/4

Fig. 9. Surface current distribution for sensor antenna at 5 GHz

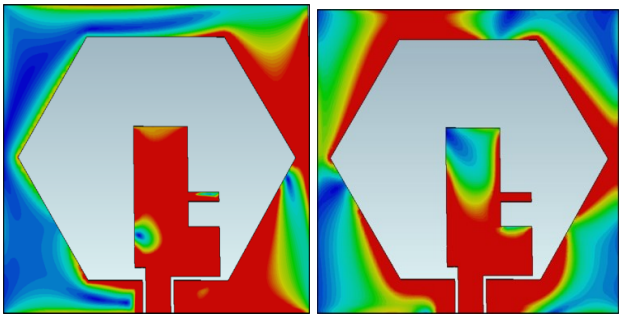

t = 0 t = T/4

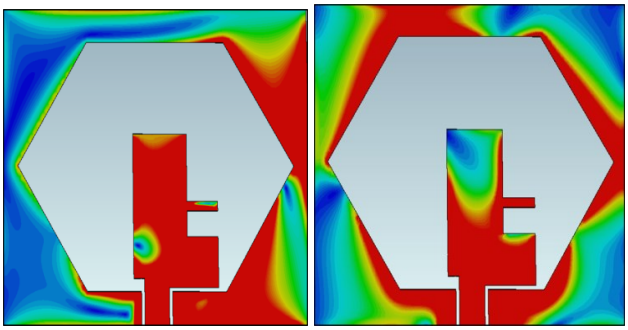

t = T/2 t = 3T/4

Fig. 10. Surface current distribution for UWB receiver antenna at 5 GHz

It can be inferred from fig. 9 and fig. 10 that only even mode [6] is generated in both the antennas. Hence, both the antennas are linear polarized and are subjected to the orientation and alignment.

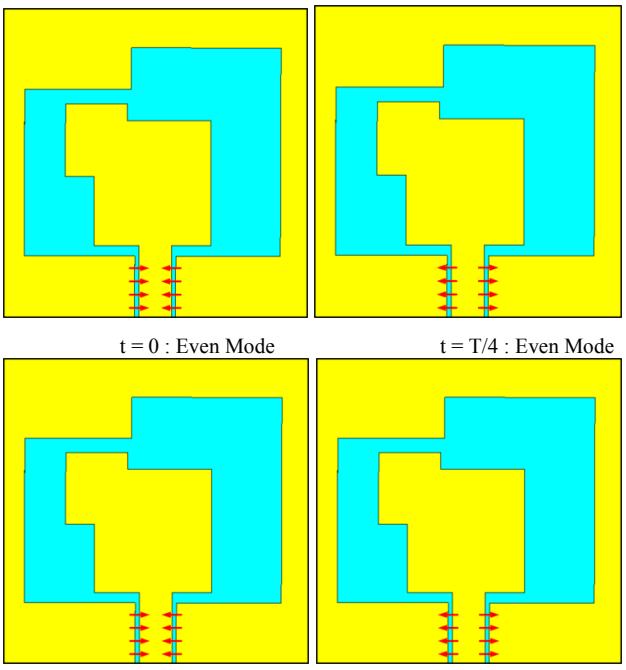

t = 0 : Even Mode t = T/4 : Even Mode

t = T/2 : Even Mode t = 3T/4 : Even Mode

Fig. 11. Mode distribution for sensor antenna at 5 GHz

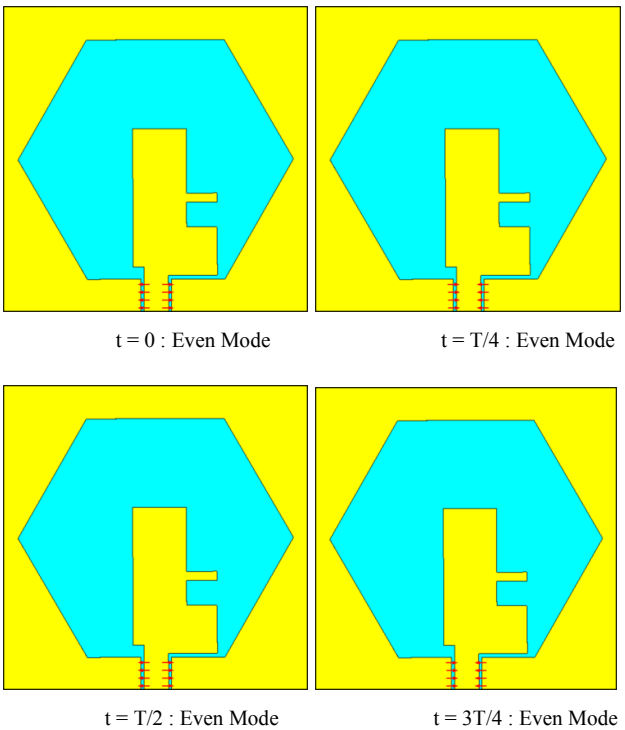

t = 0 : Even Mode t = T/4 : Even Mode

t = T/2 : Even Mode t = 3T/4 : Even Mode

Fig. 12. Mode distribution for UWB receiver antenna at 5 GHz

III. RESULTS AND DISCUSSION

A. Far Field Parameters analysis

S_{11} of the proposed sensor antenna is depicted in fig. 13, which confirms the single resonating band with center frequency at 5 GHz. Fig. 14 depicts the 10 dB impedance bandwidth of the ultra wideband antenna , which confirms that the resonating band sweeps the entire 3–12 GHz spectrum. As aforementioned, the sensor antenna resonates at 5 GHz when mounted on the surface of the test material with permittivity equals to one. Now as per the proposed concept, with the increment in the value of permittivity of the test material, the resonating band of sensor antenna must shift. This is verified in fig. 15, which illustrates that the resonating band for sensor antenna shifts towards left side with the increment in dielectric constant value of the test material. Hence, non destructive testing of the dielectric material can be carried out by this method for evaluating the healthiness of the permittivity value. Simulated average gain of the sensor antenna is shown in fig. 16, while for ultra wideband antenna it is depicted in fig. 17. 3D radiation pattern for sensor antenna is plotted in fig. 18, while radiation pattern for ultra wideband antenna is depicted in fig. 19. Radiation patterns of both the antennas confirm their directive nature.

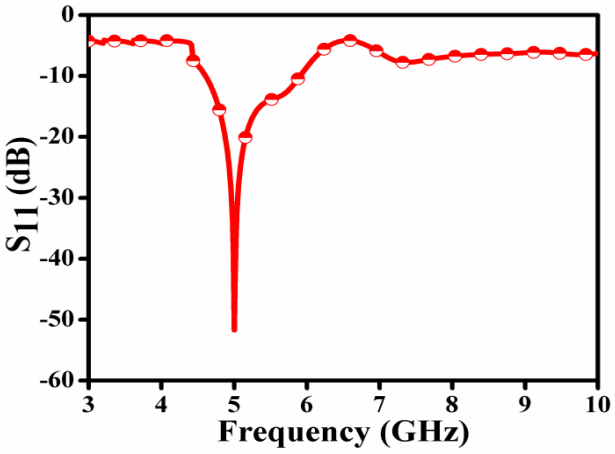

Fig. 13. S_{11} of proposed sensor antenna

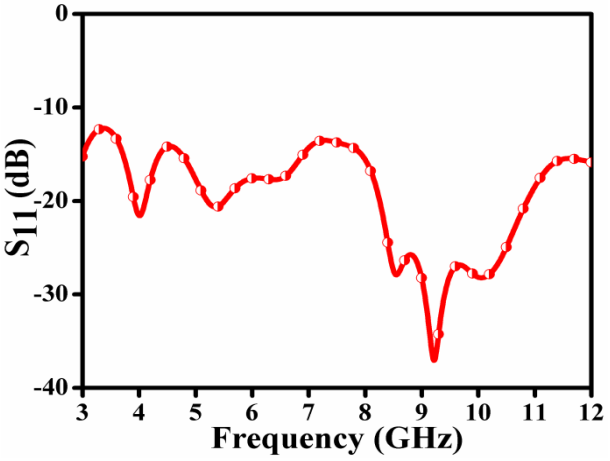

Fig. 14. S_{11} of proposed UWB receiver antenna

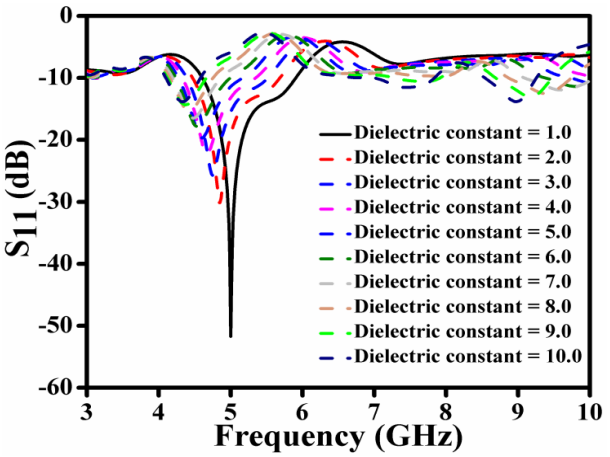

Fig. 15. Shift in resonating band of sensor antenna with increment in permittivity value of test material

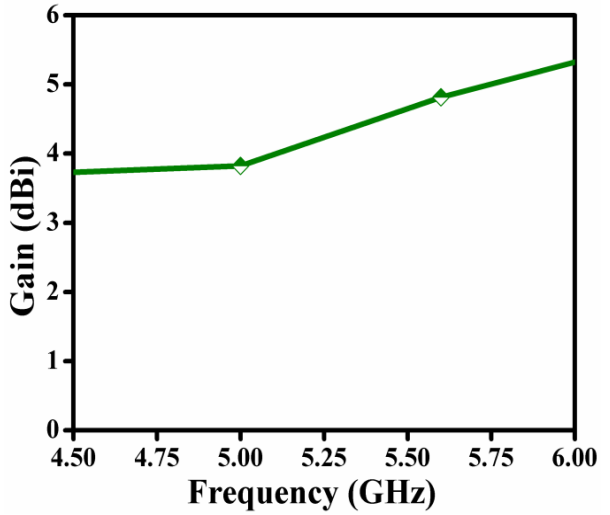

Fig. 16. Gain of proposed sensor antenna

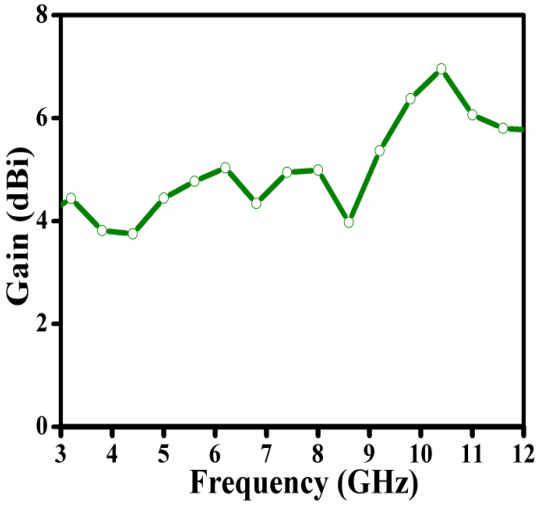

Fig. 17. Gain of proposed UWB receiver antenna

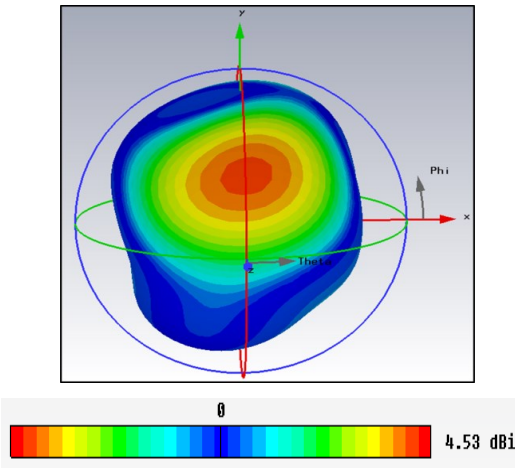

Fig. 18. 3D radiation pattern of proposed sensor antenna at 5 GHz

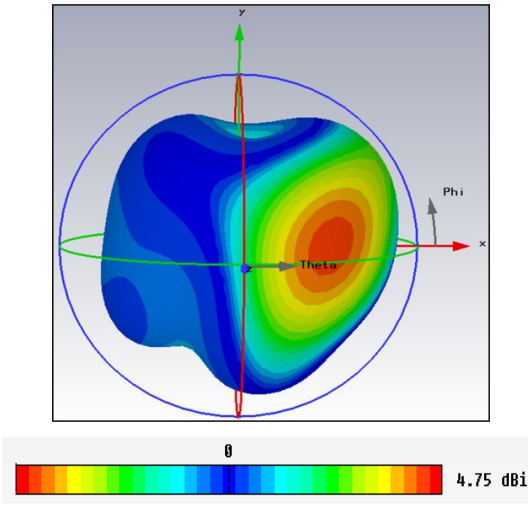

Fig. 19. 3D radiation pattern of proposed UWB receiver antenna at 5 GHz

B. Friis Equation Analysis

Friis equation analysis for the proposed antenna setup is carried out in this section in order to calculate the power received by the ultra wideband receiver antenna. It must be noted that the received power is calculated by considering 1dBm reference power transmitted by the sensor antenna. Friis equation for a dual antenna setup is illustrated as equation (1), operating wavelength of the antenna setup is calculated using equation (2), while the Far field range for the proposed setup is obtained from equation (3). P_t = 1 dBm = 1.25 mW, G_t = 3.8 dB = 2.40, G_r = 4.4 dB = 2.75, ε_r = 4.2 for FR4 substrate.

$$P_r = (P_t G_t G_r) / \text{Path Loss} \quad (1)$$

$$\Rightarrow P_r = (P_t G_t G_r \lambda^2) / (4\pi R)^2$$

$$\Rightarrow P_r = -26 \text{ dBm}$$

$$\lambda = (3 \times 10^8) / \sqrt{\varepsilon_r} \quad (2)$$

$$\Rightarrow \lambda = 0.0293 \text{ m}$$

$$R = 2 \times d^2 / \lambda \quad (3)$$

$$\Rightarrow R = 0.06 \text{ m}$$

P_t is the power transmitted by the sensor antenna, G_t is the gain of the sensor antenna, G_r is the gain of the ultra wideband reciever antenna, λ is the operating wavelength of the setup, R is the minimum Farfield distance for the proposed setup, d is the largest dimension of the sensor antenna. From equation (1) it can be inferred that for 1 dBm transmitted power by the sensor antenna, -26 dBm is the power received by the ultra wideband antenna.

IV. CONCLUSION

A dual antenna setup simulation model for non destructive evaluation of relative permittivity of dielectric material has been studied in this paper. Two antennas, namely, sensor antenna and ultra wideband receiver antenna have been proposed. The sensor antenna has a single resonating band operating at 5 GHz and is mounted on the surface of the test material. Shift in the resonating band of the sensor antenna is captured by the ultra wideband receiver antenna which reflects variations in the value of dielectric constant of the test material. The proposed simulation model can be further extended to tera hertz frequency range with adequate setup for achieving high measurement accuracy and to analyze presence of air voids along with permittivity value and its status.

REFERENCES

[1] K. T. Chandrasekaran, M. F. Karim, Nasimuddin, M. Ong and A. Alphones, "A Backward-to-Forward Beam Scanning Leaky-Wave Antenna for Non-Destructive Testing of Cracks & Corrosion in Metallic Structures under Multilayered Composites," 2018 International Conference on Intelligent Rail Transportation (ICIRT), Singapore, 2018, pp. 1-5.

[2] A. Zhuravlev, V. Razevig, M. Chizh, S. Ivashov and A. Bugaev, "Non-destructive testing at microwaves using a vector network analyzer and a two-coordinate mechanical scanner," 2016 16th International Conference on Ground Penetrating Radar (GPR), Hong Kong, 2016, pp. 1-5.

[3] A. Zhuravlev, V. Razevig, M. Chizh and S. Ivashov, "Non-Destructive testing of foam insulation by holographic subsurface radar", 9th International Workshop on Advanced Ground Penetrating Radar IWAGPR 2017, Jun. 28-30, 2017

[4] H. Wu, M. Ravan, R. Sharma, J. Patel and R. K. Amineh, "Non-Destructive Testing of Non-Metallic Concentric Pipes Using Microwave Measurements," 2020 IEEE/MTT-S International Microwave Symposium (IMS), Los Angeles, CA, USA, 2020, pp. 369-372.

[5] P. Das and S. Ray, "NDT using open-ended waveguides," 2016 International Symposium on Antennas and Propagation (APSYM), Cochin, 2016, pp. 1-4.

[6] M. N. Osman, M. K. A. Rahim, M. F. M. Yusoff, M. R. Hamid and M. Jusoh, "Dual-port polarization reconfigurable antenna using compact CPW slotline feeding structure for space-limited MIMO application," 2015 IEEE Conference on Antenna Measurements & Applications (CAMA), Chiang Mai, 2015, pp. 1-4